Analysis on the mechanical effects induced by beam impedance heating on the HL-LHC target dump injection segmented (TDIS) absorber

IOP Conf. Series: Journal of Physics: Conf. Series **1067** (2018) 062011 doi:10.1088/1742-6596/1067/6/062011

Analysis on the mechanical effects induced by beam impedance heating on the HL-LHC target dump injection segmented (TDIS) absorber

L Teofili[1,2,3], M Migliorati[1,2,3], M Calviani[3], D Carbajo[3], S Gilardoni[3], F Giordano[3], I Lamas[3], G Mazzacano[3] and A Perillo[3]

[1] Sapienza University of Rome, Rome, Italy
[2] INFN, Rome, Italy
[3] CERN, Geneva, Switzerland

E-mail: lorenzo.teofili@uniroma1.it

Abstract. The High Luminosity Large Hadron Collider (HL-LHC) Project at CERN calls for increasing beam brightness and intensity. In such a scenario, critical accelerator devices need to be redesigned and rebuilt. Impedance is among the design drivers, since its thermo-mechanical effects could lead to premature device failures. In this context, the current work reports the results of a multiphysics study to assess the electromagnetic and thermo-mechanical behaviour of the Target Dump Injection Segmented (TDIS). It first discusses the outcomes of the impedance analysis performed to characterise the resistive wall and the high order resonant modes (HOMs) trapped in the TDIS structures. Then, their RF-heating effects and the related temperature distribution are considered. Finally, mechanical stresses induced by thermal gradients are studied in order to give a final validation on the design quality.

1. INTRODUCTION

The CERN accelerator complex has been upgrading to improve its performance. In the framework of the LIU (LHC Injection Upgrade)[1] and HL-LHC (High Luminosity LHC) [2] projects an increase of the beam brightness and intensity is foreseen [1]. Several systems have to be redesigned and rebuilt to face the new situation.

Devices impedance, i.e. electromagnetic beam equipment interaction, is among the systems design drivers. This interaction causes a power deposition on the equipment (RF-Heating), proportional to the square of the beam intensity and to the device impedance [3]. The deposition, due to the presence of trapped high order modes, can be highly irregular, so leading to an uneven temperature distribution. As a result, temperature gradients may induce intense mechanical stresses causing failures or other undesired effects [4, 5].

In this context, this paper presents the results of the multiphysics simulations performed to assess the electro-thermo-mechanical behaviour of the Target Dump Injection Segmented (TDIS) [6], that could experience RF-heating as high as its predecessor, the Target Dump Injection [6, 4].

The TDIS will protect downstream LHC equipment during the injection phase, absorbing the injected beam in case of malfunctions of the injection kicker in the Super Proton Synchrotron (SPS)-to-LHC injection lines [6]. The geometry of the device is presented in Fig. 1 and described in detail in [6]. Six vertically movable jaws of different materials are the core of the TDIS. During

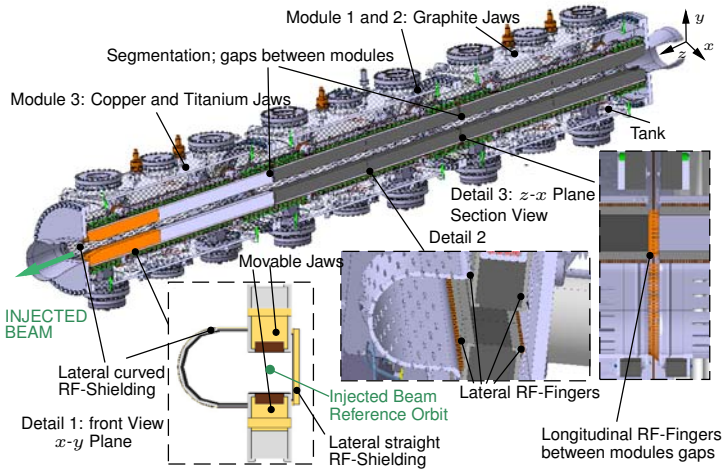

Figure 1. Geometry of the TDIS, detail on the RF-fingers configurations and transverse section.

the injection phase they have a half-gap of 4 mm with respect to the injected beam reference orbit, Fig. 2 bottom detail. Thus, if the orbit of the actual injected beam differs more than the allowed tolerance, it will impact the jaws so it is stopped. After the injection phase the jaws are completely open (half gap 55 mm).

2. METHODOLOGY

The current investigation involved electromagnetic simulations to estimate the device impedance and the associated deposited power. This power was used as an input for thermo-mechanical simulations to assess the device global behaviour.

Excluding an impact due to beam dumping, the main sources of heat loads for the TDIS are: direct beam load due to the scraping of secondary halo, and impedance heating. The latter can be further divided in resistive wall heating and HOM RF-Heating. The beam halo heat load can be easily computed analytically [7]. Regarding the impedance heating, Teofili, Lamas and Migliorati have recently proposed a method able to simulate its mechanical induced effects on a device [8]. It interfaces two commercial programs, CST Particle Studio® [9] a CERN standard for impedance computation [10, 11], and ANSYS Mechanical®[12] widely used for thermo-mechanical simulations [13, 14, 15, 16]. For this work, we adopted a slightly modified version of the method adding the contribution of the secondary halo heat load. We followed a conservative approach, considering the worst case scenario: the load of the three sources is at a maximum during the injection phase, when the jaws of the TDIS are at their minimum half-gap, 4 mm, and in the pessimistic assumption of a failure of the longitudinal RF-fingers between the jaws modules gaps (they are little silver coated beryllium-copper components which reduce device impedance guaranteeing the electrical connection among all the device parts, Fig. 1 Details). Indeed, the power deposited by the beam halos and by resistive wall effects decrease further from the beam, and in the next section we will prove that in the outlined configuration the HOM load is also maximum.

Please note that since the TDIS functional specifications are currently preliminary the outlined device characteristic could change slightly in the future. In this context, the following simulations were performed with a value of 5 mm for the minimum half gap instead of the current accepted value of 4 mm. However, this can be considered a minor deficit given the small difference between the values.

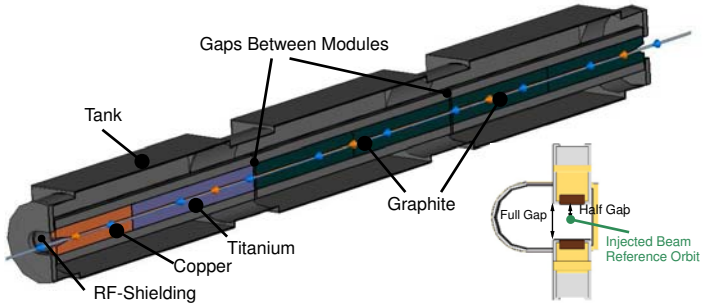

Figure 2. TDIS Model in CST.

3. ELECTROMAGNETIC SIMULATIONS

In order to evaluate the TDIS longitudinal coupling impedance and its heating effects, electromagnetic simulations were performed. The geometrical model for CST® simulations (Fig. 2), was obtained carefully simplifying the complex mechanical TDIS drawing, preserving only the features important for the electromagnetic computations, so reducing simulations time.

The TDIS was analyzed with different finger configurations and with different half-gap apertures. In Fig. 3 results of CST wakefield [17] simulations for 5 mm half-gap are reported for the cases with and without longitudinal RF-fingers with the HL-LHC beam spectrum. For the scenario with fingers, there are no trapped resonant modes inside the structure below 1.25 GHz. Indeed, electric contacts prevent trapped modes below the cutoff frequency of the LHC pipe. In the scenario without RF fingers, several trapped modes are presents below 1.25 GHz. There is a clear contribution to the longitudinal impedance in the beam spectrum frequency range. The impact of the absence of longitudinal fingers was then further investigated: the shunt impedance of every trapped mode obtained by the CST eigenmode solver [18] was compared with the results of the wakefield solver, Fig. 4. The two different methods provide similar results.

Following the conservative approach, to compute the impedance HOM deposited power we used the eigenmode results in the scenario without RF-Finger. The power was numerically computed for the HL-LHC beam following the work of Furman, Lee and Zotter [3]. Furthermore, a sensitivity analysis of the impedance induced power was performed. For each considered jaw aperture an impedance curve was estimated. The impedance peaks (i.e the high order modes)

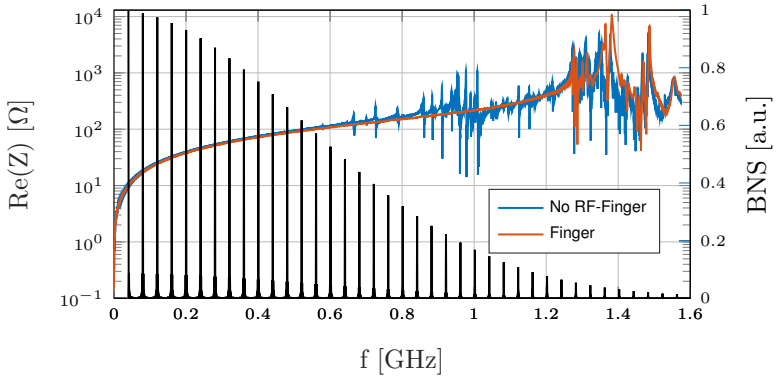

Figure 3. Beam normalized spectrum (BNS) in black and longitudinal impedance real part in log scale, 5 mm half-gap.

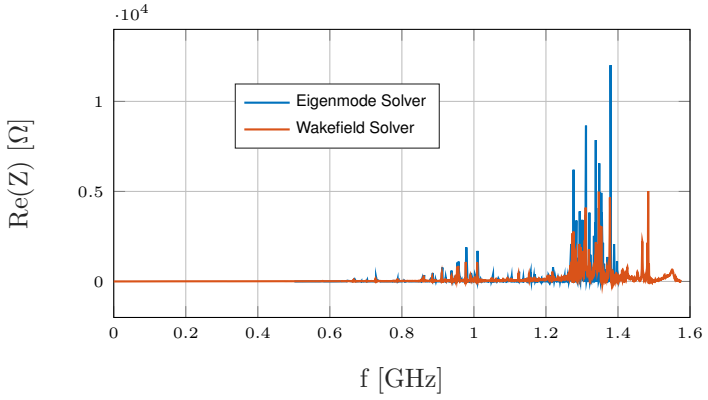

Figure 4. Longitudinal impedance real part, 5 mm half-gap.

were individually moved from their original frequencies within a range of ±10 MHz to obtain the maximum coupling with the HL-LHC beam spectrum, i.e. the maximum power loss. Figure 5 shows the HOM RF-Heating spectrum for different TDIS half-gap configurations. Despite the similar appearance, the 5 mm half gap configuration is the most critical with a total deposited power on the device of 1003 W (704 W for the 25 mm half gap case). Analyses of the resistive wall impedance heat load have demonstrated that, as expected, the worst case scenario is at 5 mm half gap with a total dissipation of 798.3 W in addition to the HOM load.

4. Thermomechanical Simulations

Following [8], the thermo-mechanical simulations on the TDIS were carried out in ANSYS®. The main goal was to verify that in the worst case scenario the TDIS local mechanical stresses were at least 20% lower than the yield (for ductile material) or the ultimate strength (for brittle material) and that the graphite blocks temperature remained below 50 °C, in order to avoid outgassing issues [20].

The heat loads considered are listed in Table 1, they occur for the duration of the injection phase (around 30 minutes) simultaneously. Other heat loads are negligible, e.g. heating effect due to e-cloud phenomena at a jaws half-gap of 5 mm [19], or not associated with the injection phase.

For the HOM RF-heating, the 3D map obtained following [8] was used. In the thermo-mechanical simulations the same geometrical model of the electromagnetic simulations was used

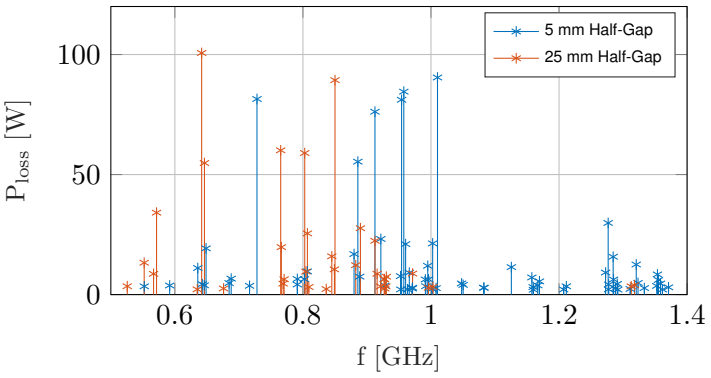

Figure 5. Power Losses due to HOMs.

Table 1. Applied Heat loads

Source	**Heat load [W]**	**Affected Element**
Secondary halos	580 [21]	Jaws free surface
Resistive Wall	798.3	Jaws free surface
RF-Heating	1003.6	Entire TDIS

with slight modifications. In particular, the RF-fingers were reintroduced in order to have a realistic representation of the contact failure case, i.e. the fingers are present in the device but they lose physical contact with device parts on their non fixed side. Both secondary halo and resistive wall impedance heating was applied as a constant heat flux on the beam facing jaws surfaces, Fig. 2. The former was considered as evenly spread on the surfaces while the latter was applied according to the resistivity of the material (i.e. 75% of the load on the jaw graphite free surfaces and 25% on the jaw titanium-copper free surfaces). The heat dissipation systems considered were: conduction, radiation, on all the free surfaces, and convection, only on the external surfaces of the tank. Furthermore, the TDIS cooling apparatus, a system of pipes identical for each jaw in which 0.135 m^3/s of water at 27 °C flows, was also simulated. The global temperature map is plotted in Fig. 6. In this figure the component with the highest temperature have been removed to optimize the scale for readability. Remarkably, the graphite remains below the 50 °C threshold.

The peak temperature at the end of the injection stage is observed on the lateral straight RF-shielding (Fig. 1 Detail 1) on the longitudinal RF contacts between the two graphite modules and is reported in Fig. 7. Regarding mechanical stresses, the maximum value is localized on the same component on which the maximum temperature develops some centimeters downstream: at the connections of the lateral straight RF-shielding with the tank, Fig. 8. This is due to the fact that the maximum temperature is at a gap. At this point the material is unconstrained and free to expand; whereas, the connection points between the tank and the straight shielding fully constraint rotational and translational degrees of freedom. This limits deformations and increases stresses on the lateral straight RF-shielding. However, the maximum Von Mises stress value is well below the yield strength of the material: 250 MPa (stainless steel 314L).

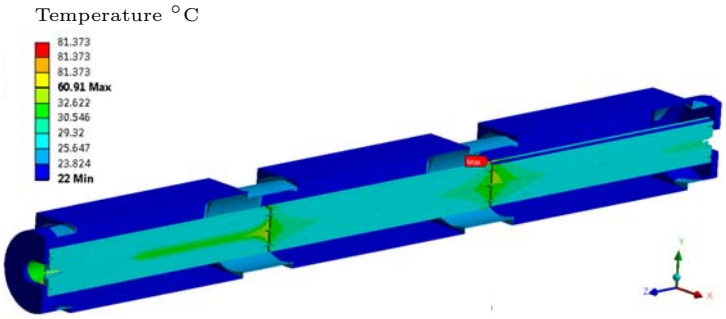

Figure 6. Global temperature distribution.

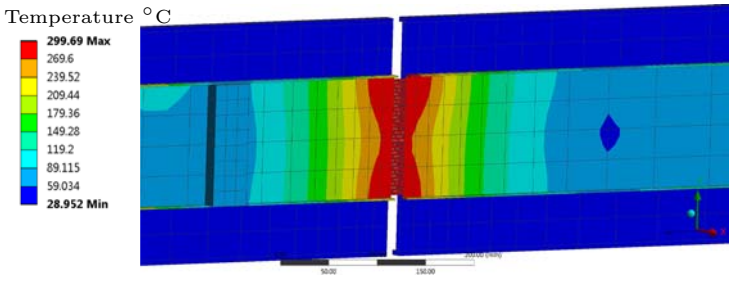

Figure 7. Temperature distribution maximum. Lateral straight RF-shielding, gap between the graphite modules.

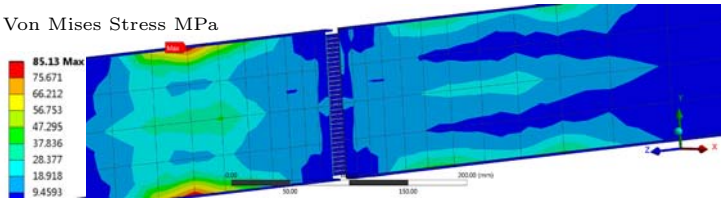

Figure 8. Stresses distribution maximum. Lateral straight RF-shielding, gap between the graphite modules.

5. Conclusions

In this study, through electromagnetic and thermo-mechanical simulations, we have assessed the quality of the TDIS design, a key component in the LHC machine, under critical working conditions. We explored its electromagnetic behaviour, we found the design robust given the absence of trapped HOM in the structure up to 1.25 GHz. We further investigated a pessimistic scenario of longitudinal RF-Fingers failure, and we explored the mechanical effects of the power deposited by the electromagnetic beam-device and nuclei-matter interactions. Despite the fact that our findings have highlighted some possible critical areas, neither the developed temperatures or the related mechanical stresses seems to be high enough to cause problems, demonstrating the high quality of the design. Future studies should adopt the final minimum half-gap and further investigate the highlighted critical zones with a more refined model to understand even better stress and temperatures distributions.

References

[1] Coupard J *et al.*, LHC Injectors Upgrade Projects at CERNMay 8-13 2016 *Proc. 7th Int. Particle Accelerator Conference (IPAC16), (Busan, Korea)* doi:10.18429/JACoW-IPAC2016-MOPOY059 URL `http://accelconf.web.cern.ch/accelconf/ipac2016/html/instdoi.htm`

[2] Apollinari G, Bejar A, Bruning O, Lamont M and Rossi L Dec. 2015 *High-Luminosity Large Hadron Collider (HL-LHC) : Preliminary Design Report*, Tech. Rep. CERN-2015-005 CERN Geneva Switzerland URL `https://cds.cern.ch/record/2116337/files/CERN-2015-005.pdf`.

[3] Furman M, Lee H and Zotter B *Energy loss of bunched beams in RF cavities* 1986 Tech. Rep. SSC-086 Lawrence Berkeley Laboratory Berkeley California URL `http://inspirehep.net/record/233670/files/ssc-86.pdf`.

[4] Salvant B *et al.* Beam Induced RF Heating in LHC in 2005 May 8-13 2016 *Proc. 7th Int. Particle Accelerator Conference (IPAC16), (Busan, Korea)* doi:10.18429/JACoW-IPAC2016-MOPOR008, URL

https://cds.cern.ch/record/2207346/files/mopor008.pdf.

[5] Lipka D Heating of a DCCT and a FCT due to wake losses in PETRAIII, simulations and solutions *presented at the Simulation of Power Dissipation & Heating from Wake Losses Workshop, Diamond Light Source, Oxfordshire, UK, Jan. 2013*, unpublished.

[6] Carbajo D *et al.* Operational Feedback and Analysis of Current and Future Designs of the Injection Protection Absorbers in the Large Hadron Collider at CERN May 14-19 2017 *Proc. of 8th Int. Particle Accelerator Conference. (IPAC17), (Copenhagen, Denmark)* doi:10.18429/JACoW-IPAC2017-WEPVA108 URL http://cds.cern.ch/record/2207470/files/thpmy019.pdf.

[7] Goddard B, Kain V and Lamont M *Function and Operating Conditions of the TDI Beam Absorber* 2004 (CERN EDMS, # 508735, pp. 8.)

[8] Teofili L *et al.* A Multi-Physics Approach to Simulate the RF Heating 3D Power Map Induced by the Proton Beam in a Beam Intercepting Device April 29 - May 4, 2018 *Proc. of 9th International Particle Accelerator Conference (IPAC18) (Vancouver, Canada)* preprint THPAK093.

[9] CST Studio Suite, URL https://www.cst.com/products/csts2

[10] Zannini C Electromagnetic Simulation of CERN accelerator Components and Experimental Applications *Ph.D. thesis, Phys. Dept., Ecole Polytechnique, Lausanne, Switzerland, 2013*, URL https://infoscience.epfl.ch/record/187002/files/EPFL_TH5737.pdf.

[11] Salvant B Impedance model of the CERN SPS and aspects of LHC single-bunch stability *Ph.D. thesis, Eng. Dept., Ecole Polytechnique, Lausanne, Switzerland, 2010*, URL https://infoscience.epfl.ch/record/142384/files/EPFL_TH4585.pdf.

[12] ANSYS, URL https://www.ansys.com/

[13] Dallocchio A Study of Thermo-mechanical effects induced in Solids by High Energy Particle Beams: Analytical and Numerical Methods *Ph.D. thesis, Phys. Dept., Politecnico di Torino, Torino, Italy, 2008*, URL https://cds.cern.ch/record/1314219/files/CERN-THESIS-2008-140.pdf.

[14] Torregrosa C Comprehensive Study for an Optimized Redesign of the CERNs Antiproton Decelerator Target *Ph.D. thesis, Eng. Dept. Universidad Politecnica de Valencia Valencia Spain, 2017*, URL https://cds.cern.ch/record/2314375/files/CERN-THESIS-2017-357.pdf.

[15] Romagnoli G *et al.* Design of the New PS Internal Dumps, in the Framework of the LHC Injector Upgrade (LIU) Project May 14-19 2017 *Proc. of 8th Int. Particle Accelerator Conference. (IPAC17), (Copenhagen, Denmark)* doi:10.18429/JACoW-IPAC2017-WEPVA109 URL http://inspirehep.net/record/1626290/files/wepva109.pdf.

[16] Lamas I *et al.*, LHC Injection Protection Devices, Thermo-mechanical Studies through the Design Phase May 8-13 2016 *Proc. 7th Int. Particle Accelerator Conference (IPAC16), (Busan, Korea)* doi:10.18429/JACoW-IPAC2016-THPMY019 URL http://accelconf.web.cern.ch/accelconf/ipac2016/papers/thpmy019.pdf.

[17] CST: Wakefield Solver, URL https://www.cst.com/products/cstps/solvers/wakefieldsolver

[18] CST: Eigenmode Solver, URL https://www.cst.com/products/cstmws/solvers/eigenmodesolver

[19] Skripka G and Iadarola G Buildup studies for the LHC TDIS URL https://indico.cern.ch/event/707491

[20] Jimenez J *Vacuum requirements for the LHC* 2003 (CERN EDMS,# 428155, p. 6.)

[21] Carbajo D, Perillo A and Teofili L private communication Nov. 2017.